Article

Conjugation of 10 kDa linear PEG onto trastuzumab Fab' is sufficient to significantly enhance lymphatic exposure while preserving in vitro biological activity

Linda J. Chan, David B. Ascher, Rajbharan Yadav, Jurgen B. Bulitta, Charlotte C. Williams, Christopher J.H. Porter, Cornelia B. Landersdorfer, and Lisa M. Kaminskas

Mol. Pharmaceutics, **Just Accepted Manuscript** • DOI: 10.1021/acs.molpharmaceut.5b00749 • Publication Date (Web): 12 Feb 2016

Conjugation of 10 kDa linear PEG onto trastuzumab Fab' is sufficient to significantly enhance lymphatic exposure while preserving in vitro biological activity

Linda J. Chan[†], David B. Ascher[‡], Rajbharan Yadav[†], Jürgen B. Bulitta[†#], Charlotte C. Williams[§], Christopher J. H. Porter[†], Cornelia B. Landersdorfer[†], Lisa M. Kaminskas[†]*

[†]Drug Delivery, Disposition and Dynamics, Monash Institute of Pharmaceutical Sciences, Monash University, 381 Royal Parade, Parkville, Victoria 3052, Australia

[‡]Department of Biochemistry, University of Cambridge, Sanger Building, Downing Site, Cambridge, CB2 1GA, U.K.

[#]Center for Pharmacometrics and Systems Pharmacology, College of Pharmacy, University of Florida, Orlando, FL, USA

[§]CSIRO Materials Science and Engineering, 343 Royal Parade, Parkville, Victoria 3052, Australia

*Corresponding author:
Dr Lisa M. Kaminskas
Drug Delivery, Disposition and Dynamics
Monash Institute of Pharmaceutical Sciences
Monash University
381 Royal Parade, Parkville
VIC 3052, Australia
Ph: +61 3 99039522
Email: lisa.kaminskas@monash.edu

Keywords: Monoclonal antibody, trastuzumab, Fab, PEGylation, lymphatic, pharmacokinetics, population modeling, S-ADAPT

For table of contents use only

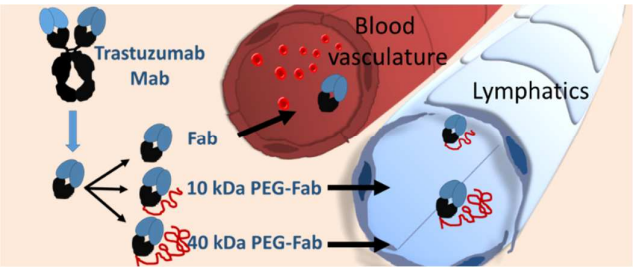

Abstract

The lymphatic system is a major conduit by which many diseases spread and proliferate. There is therefore increasing interest in promoting better lymphatic drug targeting. Further, antibody fragments such as Fabs have several advantages over full length monoclonal antibodies, but are subject to rapid plasma clearance which can limit the lymphatic exposure and activity of Fabs against lymph-resident diseases. This study therefore explored ideal PEGylation strategies to maximise biological activity and lymphatic exposure using trastuzumab Fab' as a model. Specifically, the Fab' was conjugated with single linear 10 or 40 kDa PEG chains at the hinge region. PEGylation led to a 3-4 fold reduction in binding affinity to HER2, but anti-proliferative activity against HER2-expressing BT474 cells was preserved. Lymphatic pharmacokinetics were then examined in thoracic lymph duct cannulated rats after intravenous and subcutaneous dosing at 2 mg/kg and the data were evaluated via population pharmacokinetic modelling. The Fab' displayed limited lymphatic, but conjugation of 10 kDa PEG improved exposure by approximately 11 and 5 fold after intravenous (15% dose collected in thoracic lymph over 30 h) and subcutaneous (9%) administration respectively. Increasing the molecular weight of the PEG to 40 kDa, however, had no significant impact on lymphatic exposure after intravenous (14%) administration and only doubled lymphatic exposure after subcutaneous administration (18%) when compared to 10 kDa PEG-Fab'. The data therefore suggests that minimal PEGylation has the potential to enhance the exposure and activity of Fab's against lymph-resident diseases, while no significant benefit is achieved with very large PEGs.

Introduction

Monoclonal antibodies (mAbs) are rapidly gaining momentum as a major class of pharmaceuticals that are increasingly being utilised to treat a wide range of diseases[1, 2]. Antibodies possess several desirable characteristics as therapeutic entities such as good stability, solubility, high specificity and selectivity and prolonged plasma circulation[3, 4]. Recently, we have also demonstrated that mAbs efficiently access lymph fluid after subcutaneous (SC) and intravenous (IV) administration[5, 6], highlighting their utility against diseases of, or that reside within the lymphatic system. The predominant class of antibodies used as therapeutics is IgG, which are used for many current cancer and autoimmune disease therapies. IgGs are large multimeric proteins comprised of two identical heavy chains and two identical light chains which are linked together by a series of disulfide bonds and have a molecular weight of approximately 150 kDa. They contain two distinct functional subunits; the antigen binding (Fab) and constant regions (Fc). The Fab region is composed of domains associated with the light chain (V_L, C_L) and the heavy chain (V_H, C_{H1}). The Fc portion contains the domains for the heavy chains, C_{H2} and C_{H3} and is responsible for binding to a wide range of cell-associated receptors and for enhancing the systemic exposure of mAbs[7].

In addition to full length mAbs, Fab fragments have also been developed as biological therapeutics, and several Fab-based medications are currently approved in the clinic[1]. For instance, an anti-glycoprotein IIb/IIIa chimeric Fab, abciximab is approved for clot prevention following angioplasty[8]. In 2006, ranibizumab, an anti-vascular endothelial growth factor humanized Fab was approved for use for macular degeneration[9] and certolizumab pegol (Cimzia), which is a PEGylated (40 kDa PEG) anti-tumor necrosis factor (TNF)α Fab' conjugate, is utilized for the treatment of Crohn's disease and arthritis[10]. Fab-conjugated nanoparticles and drug delivery systems are also being explored as a means to actively target loaded chemotherapeutic drugs towards solid tumors.

Fabs have several advantages over mAbs, including better penetration into tissues or tumors[2], monovalent antigen binding[11] and the ability to generate the protein using less costly prokaryotic expression systems[12]. Conversely, Fab fragments have short elimination half lives as a result of rapid in vivo degradation due in part to the lack of the Fc portion that is responsible for receptor-mediated recycling of antibodies and neonatal Fc receptor (FcRN)-mediated transfer[13, 14]. In addition, the smaller size (approximately 50 kDa) and rapid plasma clearance of Fabs is expected to limit exposure and activity against lymph-resident diseases when compared to full length mAbs. The significance of this lies in the fact that many diseases (such as cancers, tuberculosis, filariasis and HIV) proliferate within or spread via the lymphatic system, but many of the current therapies for these diseases (with the exception of full length mAbs) are directed at treating the 'systemic disease' only and do not efficiently access the lymphatics, thus restricting therapy (reviewed in [15]). Improving the lymphatic disposition of Fabs with indications against lymph-resident diseases whilst also retaining target binding affinity is therefore expected to improve activity against these diseases. Ideally, the beneficial effects that Fabs have over mAbs (such as lower manufacturing costs) would be preserved, whilst promoting similar lymphatic disposition and activity against lymph-resident diseases to the respective mAbs.

Consequently, a number of strategies have been explored to increase the in vivo stability and effective size of Fab fragments, thereby prolonging plasma exposure, including the conjugation of polyethylene glycol (PEG; PEGylation), the attachment of proteins such as albumin and more recently, PASylation[16] (the attachment of hydrophilic, small residues Pro-Ala-Ser (PAS)). PEGylation has long been the preferred approach to prolong the plasma exposure and therapeutic activity of antibodies and antibody fragments and other therapeutic proteins. As a general rule, increasing PEG loading (the proportion of a PEGylated proteins mass that is attributed to the PEG) via conjugation of larger or a greater number of PEGs increases plasma exposure. PEGylation can improve the solubility and reduce

the immunogenicity of proteins and enhance the anti-tumor activity of Fabs and other immunomodulatory proteins by prolonging systemic exposure by virtue of reducing proteolysis and renal elimination[17, 18]. Additionally, several studies have suggested that PEGylation can improve Fab uptake into solid tumors without subsequently increasing uptake into normal tissues[19-21]. More recently, it has been shown that the SC bioavailability and lymphatic disposition of therapeutic proteins can also be improved via optimal PEGylation[18].

To this end, the targeted delivery of small and macromolecular drugs to the lymphatic system is being increasingly explored as an approach to improve their exposure and activity against lymph-resident diseases. However, while the impact of PEG loading on the plasma pharmacokinetics of Fabs and other proteins has been relatively well established (reviewed in [3]), the relationship between PEG loading and lymphatic disposition is more complex. In general, small molecules are absorbed via the blood vasculature as a result of their good permeability through the vascular epithelia and faster flow (approximately 100 fold) of blood through vascular capillaries when compared to lymph through lymph capillaries. Macromolecules, however, typically display poor permeability through the vascular epithelium and are therefore more available for uptake via the lymphatic system as a result of wider interendothelial cell junctions and lack of a significant basement membrane and smooth muscle layer[15]. Thus, the lymphatic uptake of proteins from an SC injection site is correlated with molecular weight, such that larger proteins more avidly access the lymph[22]. However, by increasing the molecular weight of PEG conjugated to interferon α2 (19 kDa) from 12 kDa PEG (31 kDa construct) to 40 kDa PEG (60 kDa construct) lymphatic exposure after IV administration is increased in rats, but no further improvements in lymphatic exposure are observed after SC administration[18]. Conversely, Increasing the molecular weight of PEGylated polylysine dendrimers from 22 to 68 kDa leads to an increase in lymphatic exposure after SC administration, but similar lymphatic exposure over 30 h following IV administration[23]. In addition, 20% PEG loading (by MW) of the anti-HER2 mAb

trastuzumab has no impact on lymphatic exposure after IV or SC administration when compared to the native mAb[6].

One of the major drawbacks of PEGylation, however, is that it also typically reduces in vitro biological activity (such as receptor binding affinity), and this is generally a function of the site of PEG attachment, the number of conjugated PEGs and the overall degree of PEG loading, whereby increased PEG loading (associated with an increase in hydrodynamic volume) typically reduces biological interactions[2]. Conversely, in vivo activity is a function of both drug exposure at the target and receptor binding affinity. This study therefore sought to identify the degree of PEG loading that maximises the lymphatic exposure of Fabs at the same time as retaining binding affinity to the receptor and in vitro biological activity. In this instance, the Fab' fragment of trastuzumab was used as a model antibody fragment since we have extensive experience in evaluating the lymphatic pharmacokinetics of this mAb[5, 6]. In this study, PEGylated Fabs were prepared via the site directed conjugation of single 10 or 40 kDa linear PEGs to thiol groups present at the hinge region on the Fab' fragment. The Fab' fragment was prepared by pepsin digestion of trastuzumab followed by reduction of F(ab)'2. Reaction of Fab' with PEG-maleimide gave 10 kDa PEG-Fab (approximately 60 kDa, 20% w/w PEG loading) and 40 kDa PEG-Fab (approximately 90 kDa, 45% PEG loading). The lymphatic pharmacokinetics of the Fab' and PEGylated Fabs after SC and IV administration in rats were then evaluated as well as the HER2 binding affinity and growth inhibition of HER2-positive breast cancer cells (BT474) by each construct.

Experimental Section

Reagents and supplies: Trastuzumab (Herceptin®) was purchased from Roche Pty Ltd (Dee Why, NSW, Australia). Linear methoxy PEG maleimides (MAL-PEG-OMe, 10 kDa and 40 kDa) were purchased from JenKem Technology (Plano, TX, USA). Human breast cancer cells, BT474 cells, were kindly provided by Dr Mark Waltham at St Vincent's Institute of Medical Research (VIC, Australia). DMSO, thiazolyl blue tetrazolium bromide and 3,3',5,5'–tetramethylbenzidine (TMB) tablets were from Sigma-Aldrich (Castle Hill, NSW, Australia). Molecular weight markers and polyacrylamide gels (4-12% Bis-Tris) were purchased from Life Technologies (Mulgrave, VIC, Australia). Silastic, polyvinyl and polyethylene tubings (0.58mm internal diameter, 0.96mm external diameter) were obtained from Microtube Extrusions Pty Ltd (NSW, Australia). Recombinant human s-HER2 encoding amino acids 23 - 652 of the full length protein was purchased from Jomar Bioscience (Kensington, SA, Australia). Sterile cell culture reagents were from Gibco® Life Technologies. All other analytical grade buffer reagents were purchased from Ajax Finechem Pty Ltd (NSW, Australia) and Sigma-Aldrich (Castle Hill, NSW, Australia).

Animals: Male Sprague-Dawley rats (250-320 g) were obtained from Monash Animal Services (Clayton, VIC, Australia) and maintained in a controlled environment with a 12 h light/dark cycle. Water was provided ad libitum. Food was withheld after surgical implantation of cannulae and for 8 h post dosing, but was provided freely at all other times. All animal experimentation was approved by the Monash Institute of Pharmaceutical Sciences Animal Ethics Committee.

Preparation of Fab' fragments of trastuzumab and PEGylated Fab's (10 kDa and 40 kDa PEG-Fab's): Trastuzumab was re-constituted according to manufacturer's instructions in 7.2 mL sterile water, yielding a final concentration of 21 mg/mL. This solution was stored in working aliquots at -80°C and thawed immediately prior to use. Sterile and endotoxin-free consumables were used during the preparation and purification of Fab' and PEG-Fab's where possible. The re-constituted

trastuzumab solution was buffer exchanged into 0.1 M citrate buffer (pH 3.5) to perform a pepsin digest. Pepsin was added to trastuzumab at a ratio of 1:100 w/w to remove the Fc portion and to generate $F(ab')_2$ fragments. The reaction mixture was incubated for 1.5 h in a 37 °C water bath followed by the addition of 3 M Tris buffer (pH 8.0) to neutralise the reaction (80-90% yield). The intermediate $F(ab')_2$ fragments were then purified via size exclusion chromatography using a HiLoad Superdex 200 26/60 column and a mobile phase consisting of phosphate buffered saline (PBS) containing 0.5 mM EDTA (pH 7.2) at a flow rate of 3 mL/min. After concentration of $F(ab')_2$ (to approximately 7 mg/mL in 3-4 mL), three molar equivalents of 1 mM tris (2-carboxyethyl) phosphine (TCEP, approximately 700 µL) was added to the concentrated $F(ab')_2$ fractions for 1 h at room temperature to obtain the reduced Fab' (tmFab') fragments (yield approximately 70-90%). Iodoacetamide (0.2 M in sterile MQ water) was then immediately added to the tmFab' reaction mixture (approximately 4 mL at around 6 mg/ml protein) to give a 15 fold molar excess compared to the protein to block exposed hinge thiols from oxidation which would re-form these hinge disulphide bonds. The final product of this step is therefore representative of a 'blocked' Fab' which herein is used to refer to the unconjugated (non-PEGylated) Fab'. The Fab' fragments were then purified via size exclusion chromatography as described above. An additional sample of tmFab' solution was reacted immediately with PEG-maleimide reagents to generate the respective PEGylated species.

The 10 kDa PEG-maleimide and 40 kDa PEG-maleimide reagents were dissolved in sterile water to a working concentration of 10 mg/mL. The PEGylation of Fab' fragments was carried out by reacting the PEG-maleimide (at the working concentration) with Fab' (approximately 4 mL of 4 to 5 mg/ml protein) at a ratio of 0.75:1 molar equivalents of PEG:Fab' and incubated overnight at 4 °C without shaking (approximately 40% yield). This reaction yields a maleimide-thiol conjugate and the reaction conditions were optimised initially to favour the predominant formation of mono-PEGylated species. Building upon literature precedent it is assumed that this PEG-Fab' bond will remain intact in

vivo for the duration of these studies. Purification of both 10 kDa and 40 kDa PEG-Fab's was performed the following day using the same conditions as described above. The intermediate and final products were confirmed using non-reducing SDS-PAGE gels (shown in the supporting information). Native and PEGylated Fabs were then stored at -80°C in working aliquots and were thawed immediately prior to use.

Size exclusion chromatography – multi-angle light scattering (SEC-MALS): SEC-MALS analysis was performed to determine the experimental molecular weight of the soluble PEGylated species as previously described[6, 24]. PEG-Fab' trastuzumab (0.15 µg in 50 µL) was run on a Tosoh TSKgel SuperSW2000 4.6 X 300 mm column equilibrated in PBS at a flow rate of 0.35 mL/min using a Shimadzu LC-20AD isocratic HPLC coupled to a Dawn Heleos MALS detector and an Optilab T-rEX refractive index detector (Wyatt Technologies). Dn/dc values for the PEGylated proteins were measured experimentally under the experimental conditions using the Wyatt refractometer and were 0.174 and 0.163 for the 10 and 40 kDa PEG modified Fab's respectively. The molecular weight of the Fab' portion of the molecule and the whole PEGylated construct was determined according to the three-detector method[6] using the ASTRA 5 software (Wyatt Technologies).

Microscale thermophoresis (MST): Solution MST binding studies were performed to measure the effect of PEGylation on the binding affinity of trastuzumab Fab for HER2 using standard protocols on a Monolith NT.115 (Nanotemper Technologies)[6, 24]. The HER2 was labelled using a RED-NHS (Amine Reactive) Protein Labelling Kit (Nanotemper Technologies) which contains an NT-647 dye as per the manufacturers instructions. Labelled HER2 was mixed with either native Fab or PEGylated Fab in PBS with 0.05% Tween-20. Each replicate was undertaken using a 16 step 2-fold serial dilution series. The HER2 protein concentration (1 nM) was chosen such that the observed fluorescence was approximately 400 units at 70% LED power. The samples were loaded into standard capillaries and heated at 40% laser power (48 mW) for 30 sec, followed by 5 sec cooling. The data were normalised

against the baseline obtained in the absence of any Fab', and the maximal response obtained at the highest concentration of inhibitor. The dissociation constant K_D was obtained by plotting the normalised fluorescence (F_{norm}) against the logarithm of the concentrations of the dilution series and resulted in a sigmoidal binding curve that could be directly fitted with a non-linear solution of the law of mass action. All experiments were performed with a minimum of 3 replicates and the normalised fluorescence thermophoresis curves were analysed using GraphPad Prism (Version 6, GraphPad, San Diego, CA, USA). K_D values were compared to the non-PEGylated Fab' by t-test, with $p < 0.05$ considered to be statistically significant.

In vitro growth inhibitory activity of Fab' and PEGylated trastuzumab Fab's against HER2 positive breast cancer cells: HER2-positive human breast cancer cells (BT474) were used to assess the growth inhibitory effects of the blocked Fab' and PEGylated Fab's in vitro. Cells were maintained in RPMI medium supplemented with 10% fetal bovine serum, 10,000 U/mL penicillin, 10,000 mg/L streptomycin and GlutaMAX™ (Gibco®) and were passaged twice per week via trypsin digestion. Growth inhibition experiments were performed in 96 well microplates by seeding 10,000 cells per well in 100 µl media. Cells were allowed to adhere overnight and media was replaced the following day and 0 to 50 µg/mL of Fab' or PEGyated Fab' was added. After 5 days, cell viability was assessed via an MTT assay[25]. The absorbance values were measured using an EnSpire® plate reader (Perkin Elmer) at 590 nm. Cell viability was expressed relative to the untreated control cells (without addition of Fab') as previously described. Individual curves were fitted using a sigmoidal dose-response (inhibition) curve on GraphPad Prism Version 6.

Lymphatic pharmacokinetics of Fab' and PEGylated Fab's after SC and IV administration in rats: The pharmacokinetics of Fab' and PEGylated Fab's were assessed in four groups of rats (n=3-4 rats per group). The four groups were comprised of: (1) IV-dosed control, non-lymph duct cannulated rats; (2) SC-dosed control, non-lymph duct cannulated rats; (3) IV-dosed, thoracic lymph-duct

cannulated rats, and (4) SC-dosed, thoracic lymph-duct cannulated rats. All rats were cannulated via the right carotid artery as previously described[23] to allow serial blood sampling from freely moving animals. Animals in groups 1, 3 and 4 were also cannulated via the right jugular vein to permit IV dosing and the replacement of fluid lost via the thoracic lymph duct cannula (via constant infusion of sterile saline at a rate of 1.3 to 1.5 mL/h) in lymph duct cannulated rats. Rats in groups 3 and 4 had cannulas implanted into the thoracic lymph duct posterior to the diaphragm as described previously[23] to allow the continuous collection of lymph fluid that entered the duct posterior to the point of cannulation.

After overnight recovery from surgery, rats in groups 1 and 3 were dosed intravenously with 2 mg/kg (in protein equivalents, not of whole construct) of Fab' or PEGylated Fab's (in 1 mL sterile saline) via the jugular vein cannula over 2 mins. A t_0 blood sample (150 µL) was then collected via the carotid artery cannula immediately after the completion of the infusion. Rats in groups 2 and 4 were lightly sedated under isoflurane anaesthesia and administered 2 mg/kg Fab' or PEGylated Fab' SC just above the inner left heel in a volume of 0.5 mL/kg and a t_0 blood sample was collected immediately after dosing. Further blood samples were collected after 10, 20, and 30 min and 1, 2, 3, 4, 6, 8, 24 and 30 h for all rats. Additional blood samples were collected at 48 and 72 h for control rats dosed with Fab' and PEGylated Fab' and also at 96, 120 and 144 h for control rats dosed with PEGylated Fab's. Lymph fluid was collected continuously from lymph duct cannulated rats (groups 3 and 4) over the following times: 0-1, 1-2, 2-3, 3-4, 4-6, 6-8, 8-12, 12-24, 24-27, and 27-30 h as described previously[6]. Control rats administered Fab' were euthanized after 3 days, while control rats administered PEGylated Fab' were euthanized after 5 days due to the longer circulation times of the PEGylated species. Lymph duct cannulated rats were euthanized after 30 h, since significant loss of plasma proteins occurs beyond this time which could impact on pharmacokinetics and lymphatic recovery of administered macromolecules as described previously[6]. All blood and lymph samples were collected

into heparinised tubes. Plasma was obtained via centrifugation of blood samples at 3,500 *g* for 5 min. All plasma and lymph samples as well as standard samples prepared in plasma and lymph on the day of dosing were stored at -20 °C prior to analysis.

Quantification of Fab' and PEGylated Fab's in plasma and lymph: Fab' and PEGylated Fab's were quantified using an ELISA based on the binding of Fab' to HER2[26] with modification. Specifically, a 100 µL aliquot of HER2 protein (0.5 µg/mL in PBS) was added to each well of a 96-well microplate (Medisorp, Nunc) and left overnight at 4°C. The HER2 protein solution was removed the following day and wells were washed twice with 200 µL PBS. Wells were then blocked with 200 µL of blocking buffer (pH 7.4 PBS containing 1% bovine serum albumin and 0.05% Tween-20) for an hour at room temperature. Each well was then washed five times with PBS containing 0.05% Tween-20 (PBS-Tween) prior to the addition of 100 µL of standards or samples. Standards (0.31 to 160 ng/mL) and samples were prepared in blocking buffer with the standards prepared in a 1:100 dilution of either plasma or lymph which was important to avoid matrix effects in the assay. Appropriate dilutions (1:100 to 1:1,000) were used to dilute plasma and lymph samples. Standards and samples were then added in 100 µl aliquots in duplicate to wells and incubated for 2 h at room temperature. Wells were washed five times with PBS-Tween before the addition of 100 µL of secondary antibody per well (anti-human IgG (Fab specific)-peroxidase at 1:5,000 dilution) for 1 h at room temperature. After washing, a 100 µL aliquot of TMB reagent was added, followed by 100 µL of 1M phosphoric acid after 20 mins to stop the reaction. The absorbance was measured at 450 nm using an EnSpire® plate reader.

Noncompartmental pharmacokinetic analysis: Noncompartmental analysis for all three compounds was performed using WinNonlin® Pro (Version 5.3, Pharsight Corp., Mountain View, CA) as described previously[5, 6]. The linear-up / log-down trapezoidal rule was used to calculate the area under the plasma concentration time curves. For groups of rats whose data allowed a reliable

estimation of the terminal half life, the area under the plasma concentration time curve from time zero to infinity was reported.

Population pharmacokinetic modelling: Population modeling was applied to compare the absorption and disposition kinetics of all three compounds by simultaneously modeling all of the plasma and lymph data. This modeling approach allowed prediction of the concentration *vs.* time profiles of each compound in plasma and lymph for normal and lymph cannulated rats.

The lymphatic exposure of Fab' and PEGylated Fab's in control and lymph duct cannulated rats after IV and SC administration were predicted using the Berkeley Madonna software (version 8.3.18) to simulate the extensive distribution of Fab' transfer into lymph as described previously.[27] Based on our previously published model structures for trastuzumab and PEG-trastuzumab in rats[5, 6], the current model was developed and refined to simultaneously describe the pharmacokinetics of the Fab' and PEGylated Fab' constructs. The same structural model was utilized for all compounds, but the parameter estimates were allowed to differ between compounds. After SC injection, a fraction of the dose was assumed to enter the central compartment (F_{PL}) and another fraction to enter the posterior, peripheral lymph compartment (F_{LY}) *via* first-order kinetics. The differential equations for the amounts of Fab' at the SC injection site that enter the central compartment (A1a) or the posterior, peripheral lymph compartment (A1b) were:

$$\frac{dA1a}{dt} = -k_{1a2} \cdot A1a \qquad \text{Initial condition (IC): } A1a_0 = F_{PL} \cdot Dose_{SC} \qquad (1.)$$

$$\frac{dA1b}{dt} = -k_{1b4} \cdot A1b \qquad \text{IC: } A1b_0 = F_{LY} \cdot Dose_{SC} \qquad (2.)$$

The rate constants k_{1a2} and k_{1b4} determined the half-lives of absorption of the Fab's from the injection site compartments A1a and A1b. The differential equations for the amount of Fab's in the central (A2) and peripheral compartments (A3) were (all initial conditions set to zero):

$$\frac{dA2}{dt} = R(1) + k_{1a2} \cdot A1a - (CL + CL_D) \cdot C2 + CL_D \cdot C3 - (k_{24} + k_{26}) \cdot A2 + k_{52} \cdot (1 - Cann) \cdot A5 + k_{72} \cdot A7 - k_{on} \cdot R9 \cdot C2 \cdot V_1 + k_{off} \cdot DR \cdot V_1 \quad (3.)$$

$$\frac{dA3}{dt} = CL_D \cdot (C2 - C3) \quad (41)$$

The Fab's in the central compartment could either distribute (CL_D) into the peripheral compartment (A3) or the peripheral lymph compartments (A4 and A6; rate constants: k_{24} and k_{26}), were eliminated via a first-order clearance (CL), or subject to target-mediated drug disposition (TMDD; described in more detail below)[28, 29]. The R(1) is a time-delimited zero-order infusion rate. The variable Cann defines a switch which collects the total amount of Fab's leaving the posterior, central lymph compartment for lymph duct cannulated rats (if Cann equals 1). If Cann is set to 0 to reflect non-lymph duct cannulated rats, there is no lymph collection and all Fab' molecules enter the central compartment.

The differential equations for the posterior, peripheral lymph (A4), the posterior, central lymph (A5) and the collected lymph compartment (A8) were (all initial conditions set to zero):

$$\frac{dA4}{dt} = k_{1b4} \cdot A1b + k_{24} \cdot A2 - k_{45} \cdot A4 \quad (52)$$

$$\frac{dA5}{dt} = k_{45} \cdot A4 - k_{52} \cdot A5 \quad (6.)$$

$$\frac{dA8}{dt} = Cann \cdot k_{52} \cdot A5 \quad (73)$$

While the Fab's are always leaving the posterior, central lymph compartment (A5), the Fab's either get collected in lymph duct cannulated animals (Cann = 1) in the A8 compartment or enter the central compartment (Cann = 0). The differential equations for the anterior, peripheral lymph (A6) and anterior, central lymph compartment (A7) were:

$$\frac{dA6}{dt} = k_{26} \cdot A2 - k_{67} \cdot A6 \quad (84)$$

$$\frac{dA7}{dt} = k_{67} \cdot A6 - k_{72} \cdot A7 \quad (9.)$$

As Fab's distributing through the anterior lymph loop were not quantified, the model was simplified by assuming that the rate constant values for the anterior and posterior lymph loops were the same.

A TMDD model[28, 29] was considered to describe a time-dependent binding of antibody fragments (especially the blocked, unPEGylated Fab'). The antibody fragments were assumed to bind to a receptor (R, compartment 9) and form a drug-receptor complex (DR, compartment 10). This binding was assumed to be reversible and described by rate constants k_{on} and k_{off}. Receptor synthesis was described by a zero-order rate (k_{syn}). Degradation of the receptor (k_{deg}) and of the drug-receptor complex (k_{int}) were described by first-order rate constants. The differential equations for the receptor compartment (R) and drug-receptor complex compartment (DR) were:

$$\frac{dR}{dt} = k_{syn} - k_{deg} \cdot R - k_{on} \cdot R \cdot C2 + k_{off} \cdot DR \quad (105)$$

$$\frac{dDR}{dt} = k_{on} \cdot R \cdot C2 - \left(k_{off} + k_{int}\right) \cdot DR \quad (116)$$

The C2 and C3 were modeled in units of mg/L and it was assumed that R and DR were in mg/L. Therefore, the terms from equation (10) were multiplied with V1 to obtain the appropriate units (mg/h) for equation (3).

The between subject variability of the estimated population pharmacokinetic parameters was assumed to be log-normally distributed. The residual unidentified variability was described by a combined additive and proportional error model for both plasma and lymph. The applied population analyses were performed in the parallelized S-ADAPT software and used the same estimation methods and population model diagnostics as those described previously[30-32]. The plasma concentrations and fractions of dose excreted into lymph were fitted during each dosing interval as described previously[5, 6]. Additionally, the fractions of dose excreted cumulatively into lymph were

plotted. The lymphatic exposure of both Fab' and PEGylated Fab's in control and lymph duct cannulated rats after IV and SC administration were predicted using the Berkeley Madonna software (version 8.3.18) to simulate the extensive distribution of Fab' transfer into lymph as described previously[5].

Statistical Analysis: The noncompartmental pharmacokinetic parameters for PEG-Fab' constructs were compared using one-way ANOVA. Plasma concentration-time profiles of Fab' and PEG-Fab' constructs in control and lymph cannulated rats post IV or SC dosing were compared via two-way ANOVA with Bonferroni's test at each time point. Significance was at a level of $p < 0.05$.

Results

Preparation and characterisation of blocked trastuzumab Fab' and PEGylated Fab's (10 kDa and 40 kDa PEG-Fab's): Blocked Fab' fragments were successfully prepared by capping free thiol residues in the cleaved hinge region with iodoacetamide. PEG-Fab' conjugates containing either 10 kDa PEG or 40 kDa were prepared using maleimide-terminated PEGs. Conjugation reactions occurred by reaction of the maleimide with free thiols present on the 'un-blocked' Fab' fragments (Figure 1). The conjugation of a single PEG to this site was employed specifically to limit the ability of the PEG to block the binding site of the Fab', thus maximizing in vitro biological activity of the PEGylated species. The synthesis and purification of Fab' and mono PEGylated Fab's were confirmed by SDS-PAGE and SEC-MALS. The final products obtained corresponded to a single band on SDS-PAGE (protein staining by Coomassie, followed by PEG staining with barium iodide). The SDS-PAGE gel of the PEG-Fab' conjugates submitted to reducing running conditions showed reduction of the Fab' interchain disulfide bonds. This confirmed the presence of both heavy and light chains from PEG-Fab' conjugates containing either 10 kDa and 40 kDa PEGs, with the PEG conjugated to the heavy chain (supporting information).

The size and polydispersity of fab' and PEGylated Fab's were examined via SEC-MALS. The average total molecular mass (Mw) of the Fab' as determined by SEC-MALS was 48,100 ± 0.1% g/mol, consistent with the molecular weight calculated from the protein sequence (approximately 49 kDa). The polydispersity ratio of the Fab' was 1.01, indicating a narrow mass distribution and no observable aggregates. The molar mass determined from the light scattering intensity using the concentration measured by differential refractive index for the 10 kDa and 40 kDa PEGylated Fab's (59,000 ± 1.4% g/mol and 92,000 ± 2.2% g/mol respectively), and the absorbance at 280 nm for the protein component (48,000 ± 0.3% g/mol and 49,000 ± 0.6% g/mol respectively) are shown in Figure 2. The experimentally measured masses of the protein were consistent with the unmodified protein. The difference in the masses calculated from absorbance and refractive index (11,000 and 43,000 g/mol) can be attributed to PEGylation and are consistent with a singly adducted species.

HER2 binding affinity of Fab' and PEGylated Fab's: MST analysis of the relative binding affinity of Fab' and PEGylated Fab's (Figure 3) showed that the Fab' binds HER2 with a KD of 0.6 ± 0.04 nM. Following PEGylation, the affinity of the Fab' for HER2 decreased by approximately 3 to 4-fold (KD = 1.6 ± 0.09 nM and KD = 2.3 ± 0.18 nM, for 10 kDa PEG-Fab' and 40 kDa PEG-Fab' respectively; two tailed t-tests compared to Fab, $p < 0.01$).

In vitro growth inhibition of HER2 expressing breast cancer cells by Fab' and PEGylated trastuzumab Fab's (10 kDa and 40 kDa): Fab' and PEGylated Fab's inhibited the growth of HER2 positive BT474 cells over 5 days in a concentration dependent manner, although maximal growth inhibition was limited to 40-60% (Figure 4) when compared to approximately 20% for the mAb[6]. The calculated IC_{50} for the Fab' was 0.7 ± 0.2 µg/mL when compared to approximately 0.4 µg/mL for trastuzumab mAb[6]. Interestingly, PEGylation did not have a significant impact on the anti-proliferative activity of the Fab', and IC_{50} values for the 10 kDa and 40 kDa PEG-Fab's were 0.4 ± 0.2 µg/mL and 0.7 ± 0.2 µg/mL respectively.

Noncompartmental lymphatic pharmacokinetics of Fab' and PEGylated Fab's: Following IV administration of Fab' to non-lymph cannulated (control) rats, plasma concentrations decreased with a terminal half life of approximately 2 h such that plasma concentrations of Fab' were below the level of accurate quantification by 24 h post dose (Figure 5A, Table 1). PEGylation, however, significantly reduced plasma clearance such that terminal half-lives of the 10 kDa PEG-Fab' and 40 kDa PEG-Fab' were approximately 24 h and 32 h respectively (Figure 5B& C, Table 1). Plasma clearance after IV administration of Fab' did not differ significantly between lymph cannulated and non-lymph cannulated rats (Figure 5A), consistent with the lack of significant lymphatic exposure for the Fab' after IV administration (Figure 6A). While the AUC^{0-30h} did not differ significantly between lymph cannulated and non-lymph cannulated rats administered 10 kDa PEG-Fab' (Table 1), plasma concentrations were slightly (but not significantly) lower in the lymph cannulated group after 24-30h (Figure 5B). This was suspected to be due to the improved transfer of 10 kDa PEG-Fab' into lymph (15% over 30 h) when compared to Fab' (Figure 6A). In contrast, the AUC^{0-30h} for 40 kDa PEG-Fab' after IV administration in lymph cannulated rats was less than half the value in non-lymph cannulated rats as a result of the significant lymphatic uptake of the construct (Table 1, Figure 5C, Figure 6).

After SC administration of Fab' and PEGylated Fab's absorption from the injection site appeared to be incomplete as evidenced by lower $AUC^{0-\infty}$ values after SC dosing when compared to IV dosing (approximately 30-50% of IV AUC, Table 1). C_{max} and T_{max} were increased with increasing molecular weight for the Fab' constructs along with AUC (Table 1). The Fab' was cleared rapidly (Cl/F) after SC administration and as a result, plasma profiles between lymph cannulated and non-lymph cannulated rats did not differ significantly (Table 1, Figure 5D). Approximately 6% of the Fab' was recovered in thoracic lymph over 12 h, but after this point Fab' could not be detected in lymph (Figure 6B). Following SC administration of the PEGylated Fab's to lymph cannulated rats, plasma concentrations from 6-30h were significantly lower than in control, non-lymph cannulated rats

(Figure 5E&F). This suggested significant lymphatic uptake of the PEGylated Fab's from the SC injection site, since dose absorbed from the SC injection site via the lymphatics is removed from lymph duct cannulated rats and delivery into the systemic circulation is prevented. In contrast, the lymph-blood circuit is preserved in control, non-lymph duct cannulated rats. Cumulative lymph profiles after SC administration, however, were interesting and suggested more rapid uptake of Fab' into lymph when compared to 10 kDa PEG-Fab' (Figure 6B). Whilst Fab' could not be quantified in lymph beyond 12 h, uptake of the 10 kDa PEG-Fab' into lymph showed no evidence of slowing by 30 h post dose. As a result, the 10 kDa PEG-Fab' did not display significantly better uptake into lymph by 30 h when compared to Fab' (Figure 6B). In contrast, approximately two-fold more 40 kDa PEG-Fab' was recovered in 30 h thoracic lymph when compared to Fab' and 10 kDa PEG-Fab' (Figure 6B).

Population pharmacokinetics: The noncompartmental pharmacokinetic data suggested that PEGylation had profound effects on the lymphatic pharmacokinetics of Fab's, but interpretation of the data was limited by the 30 h experimental time frame in lymph cannulated rats. We therefore used population pharmacokinetic modelling to simultaneously fit the plasma concentrations and amounts in lymph for all three Fab' constructs and enable simulation of the amounts in plasma and lymph in lymph cannulated rats beyond 30 h. To this end, we refined our previously reported PK model[6] to fit the Fab' data (Figure 7). Individual fits for each rat are shown in the supporting information. The final population mean parameter estimates and their biological variability between individual rats (between subject variability, BSV) are presented in Table 2. While absorption from the SC injection site was described by Michaelis-Menten kinetics for trastuzumab[5], the absorption of the Fab' constructs was described by first-order kinetics. The flexibility of the absorption model was increased by estimating the fraction of the SC dose that entered the central (F_{PL}) and posterior peripheral lymph compartments (F_{LY}) along with the respective absorption half lives that are presented as mean transit times in Table 2. This absorption model yielded a significant improvement

for the 40 kDa PEG-Fab' (p = 0.002; likelihood ratio test) and the Fab' (p = 0.012), but not for the 10 kDa PEG-Fab'. The rate of absorption from the SC injection site into the central compartment decreased with increasing molecular mass, i.e. the mean transit time was 7-fold slower for the 10 kDa PEG-Fab' and 100-fold slower for the 40 kDa PEG-Fab' than blocked Fab'.

The volume of distribution of the central compartment (V_1) was similar across all three constructs. However, the PEG-Fab's were estimated to have a smaller peripheral volume of distribution (V_2) than the Fab'. The first-order elimination from the central (plasma) compartment (i.e. CL) was significantly decreased for both PEG-Fab's, specifically clearance was 142-fold lower for the 40 kDa PEG-Fab' compared to Fab' in non-lymph cannulated rats (Table 2). This was consistent with the findings for total body clearance calculated by noncompartmental analysis (Table 1). A model that only contained the first-order elimination clearance yielded substantially biased individual and population fits for Fab'. Inclusion of target-mediated drug disposition (TMDD) in the model removed this bias and was highly significant ($p < 0.0001$; likelihood ratio test; for a model of all Fab data, but no data on PEGylated Fab').

The model estimated in vivo binding constants revealed that the Fab' (k_{on}: 2.69 L/mg·h) had very high binding affinity towards the HER2 receptor compared to binding constants for other two PEG-Fab's (k_{on} : 0.0158 L/mg·h for 10 kDa PEG-Fab' and 0.0126 L/mg·h for 40 kDa PEG-Fab'). The dissociation half life was 4-fold longer for Fab' compared to the PEGylated constructs (Table 2). The rates of receptor degradation (k_{deg}) and complex elimination (k_{int}) were similar (Table 2). This model yielded unbiased and reasonably precise individual and population fits for plasma concentrations and the fractions of dose collected in lymph (Figure 5 and supporting information).

The model included direct absorption of all Fab' constructs from the SC injection site into the posterior lymph compartment (MTT_{1b4}, Figure 7, Table 2). The fraction of the dose entering the lymph after SC dosing, F_{LY} (Table 2), increased with molecular mass. The rate of absorption from the

SC injection site into posterior peripheral lymph was approximately 5-fold slower for both PEG-Fab's compared to Fab'. The transit from peripheral into central posterior lymph (MTT_{45}) was slower for the PEG-Fab's than Fab' (Table 2). Transit from the central (plasma) compartment to the peripheral posterior lymph (MTT_{24}) was similar for Fab' and the 10 kDa PEG-Fab' and was approximately 5-fold slower for the 40 kDa PEG-Fab' (Table 2).

The simulated fraction of PEGylated Fab's (Table 3) flowing through the posterior lymph loop for up to 28 days after administration was 16.1% for IV dosed rats and 20.0% for SC dosed rats administered 10 kDa PEG-Fab'; and 19.1% for IV dosed rats and 41.0% for SC dosed rats administered 40 kDa PEG-Fab'. Conversely, in control, non-lymph duct cannulated rats, the fraction of dose flowing through the posterior lymph loop was 19.1% for IV dosed rats and 23.6% for SC dosed rats administered 10 kDa PEG-Fab'; and 23.8% for IV dosed rats and 48.6% for SC dosed rats administered the 40 kDa PEG-Fab'. The fractions of dose flowing through the posterior lymph loop were much lower for Fab' compared to the PEGylated Fab's. This was due to the extravasation of the PEG-Fab's from blood and subsequent uptake into the lymphatics.

Discussion

Antibody-based therapies are increasingly being used in the treatment of a wide range of illnesses, although the high cost of manufacture can be prohibitive in some cases. While Fabs have a number of advantages over full length mAbs, including reduced manufacturing costs[2], they exhibit much shorter plasma circulation times and (often) reduced receptor binding affinities, factors that collectively reduce therapeutic activity when compared to mAbs. To this end, plasma exposure and in vivo activity of Fabs can be improved via PEGylation. In some cases, however, there may also be significant benefit in promoting improved Fab exposure and activity more specifically in the lymphatics. For instance, one of the main uses for antibody-based therapies is currently the treatment of cancer. It is well known that a large proportion of aggressive cancers reside within or

metastasize via the lymphatics after first arresting within sentinel lymph nodes that drain the primary tumor[33]. There is also considerable worldwide research effort being placed in the development of antibody-based therapies and vaccines for HIV infection which proliferates within the lymphatics[34, 35]. The aim of this work was therefore to evaluate and identify ideal PEGylation strategies that may be used to optimize the lymphatic exposure and activity of Fabs against lymph-resident diseases. To this end, we used trastuzumab Fab' to explore the impact of minimal and more extensive PEG loading on the receptor binding affinity, in vitro growth inhibitory activity and lymphatic pharmacokinetics of Fab's.

The intrinsic binding affinity of the Fab' to the HER2 receptor was similar to the parent mAb[6] and conjugation of a single chain 10 or 40 kDa PEG to the Fab' fragment reduced HER2 binding affinity by 3-4 fold respectively when compared to the unconjugated Fab'. This suggested that conjugation of the larger PEG did not have a significant impact on receptor binding affinity when compared to the smaller 10 kDa PEG-Fab'. This was consistent with previous observations by Khalili and colleagues[26] who reported similar binding affinities for trastuzumab Fab, Fab' and full length trastuzumab mAb using an ELISA based assay. Further, they showed that the binding affinity of a 20 kDa PEG modified Fab was reduced only by approximately 2 fold. Interestingly, however, these authors also showed that the binding affinity of bevacizumab Fab was approximately 4 to 5-fold lower when compared to the full length mAb, suggesting that the impact of Fab PEGylation on binding affinity is likely to differ depending on the antibody target.

In contrast to the binding affinity data (showing similar receptor binding affinity for the Fab' and mAb), the Fab' fragments were generally less able to inhibit the growth of BT474 breast cancer cells in vitro when compared to the parent antibody[6] (with a lower maximal inhibitory affect). Interestingly, though, while PEGylation reduced the receptor binding affinity of the Fab', the anti-proliferative activity of the PEGylated Fab's did not differ when compared to Fab'. A complete

explanation for the relatively robust anti-proliferative effect of the PEGylated fragments (compared to the unconjugated Fab') is not evident at this time, but may reflect differences (i.e. a reduction) in in vitro degradation of Fab' following PEGylation. Another explanation may be changes to the intracellular trafficking and disposition of PEGylated Fab's when compared to Fab'. For instance, previous work using the full length trastuzumab antibody revealed that mAb PEGylation may alter patterns of intracellular trafficking and disposition, and in doing so, promote intracellular retention and anti-proliferative activity against BT474 cells[6]. This was previously suggested to reflect PEGylation of the Fc portion of the mAb and reduced FcRn-mediated recycling to the plasma membrane. Whilst Fab' fragments do not contain an Fc site, the current data suggest that the cellular trafficking of PEGylated Fab's may also be altered such that PEGylation does not negatively impact on in vitro antiproliferative activity, despite reduced receptor binding affinity. Thus even the highly PEGylated trastuzumab Fab' (up to 45% PEG loading) appeared to retain good in vitro biological activity when compared to the Fab' and parent mAb. Under these circumstances, in vivo biological activity might therefore be expected to be largely a function of plasma exposure (for systemic disease) or lymphatic exposure (for lymph-resident disease), or a combination of these factors.

The changes in pharmacokinetic behavior of trastuzumab Fab' after PEGylation with the two different PEG sizes were then evaluated in rats and the data was subjected to a population PK modeling approach based on our previously published work[5, 6]. SECTION REMOVED. In general, PEGylation markedly improved the pharmacokinetic behavior of the Fab' fragment in plasma and exposure was greatly extended after IV and SC administration. Since the PK model suggested that the contribution of TMDD to plasma pharmacokinetics was much less pronounced for the PEGylated Fab's when compared to Fab', the PEG molecule likely provided a form of shielding that reduced enzymatic degradation of the protein which contributed to the more prolonged plasma exposure. This was consistent with observations reported by others for a range of Fab's. Chapman *et al.*[3] , for

instance, showed that PEGylation prolongs the plasma exposure of Fab', such as certolizumab, where increases in PEG loading (via conjugation of additional PEG chains) increased plasma terminal half life. However, increased PEG conjugation typically leads to a significant and progressive reduction in in vitro biological activity by increasingly masking receptor binding sites which may limit in vivo activity. The results of the present study suggest, however, that this can be circumvented by the conjugation of single PEGs of higher molecular weight. Thus, site-specific conjugation of PEGs (for instance at free thiol groups present in the hinge region) was expected to further improve in vitro biological activity, since this limits masking of the binding region by the PEG.

After SC administration, the bioavailability of Fab' and PEGylated trastuzumab Fab's was incomplete in rats (approximately 30-50%), although this was unlikely to be due to non-linear pharmacokinetics since the plasma concentrations in the elimination phase after SC and IV administration were similar. In contrast, the SC bioavailability of the PEGylated Fab' certolizumab pegol in humans is approximately 80%. Notably, however, there is little data available on the subcutaneous bioavailability of antibodies and antibody fragments for comparison. This is likely due to the fact that antibody-based therapeutics are mainly administered intravenously due to the typically high doses and volumes that need to be injected. Coadministration with hyaluronidase, however, can circumvent this limitation and enable the comfortable administration of large volumes[36]. The mechanism by which hyaluronidase exerts this effect is by degrading hyaluronan in the interstitial space, allowing injected solutions to disperse more freely through the interstitium.

Subsequent evaluation of lymphatic transport of the Fab's in a thoracic lymph duct cannulated rat model revealed that redistribution of Fab' into the lymph after IV dosing was extremely low (approximately 1%), but was significantly enhanced by approximately 11-13 fold (based on compartmental data) for both PEGylated Fab's. This was broadly consistent with previous observations for PEGylated dendrimers[25], antibodies[6] and interferon[18] which suggested that

lymphatic exposure after IV administration of macromolecules is largely a function of plasma exposure and therefore the available time for extravasation and lymphatic reuptake. Interestingly, however, while the 40 kDa PEG-Fab' displayed more prolonged plasma exposure than the 10 kDa PEG-Fab', lymphatic exposure was not significantly enhanced after IV administration. While the reason for this is unclear at this time, the PK model suggested that the mean transit time for 40 kDa PEG-Fab' from the plasma to peripheral lymph was considerably slower than the 10 kDa PEG-Fab', likely due to its larger size and limited capacity for extravasation.

For PEGylated macromolecules and Fabs that display good absorption from SC injection sites and also display prolonged plasma circulation, whole body lymphatic exposure is therefore also expected to be high. This must be viewed with the caveat, however, that while PEGylation prolongs plasma exposure it also slows the transit of Fab's from plasma to peripheral lymph, and to a lesser extent, from peripheral lymph to central lymph. This ultimately means that lymphatic access will be delayed for PEGylated Fab's when compared to unconjugated Fab's which was also evident from the cumulative lymph uptake profiles (Figure 6).

After SC administration, Fab' showed only 6% uptake into lymph (approximately 5-10% of the absorbed dose based on noncompartmental and compartmental data). Minimal PEGylation (approximately 20% PEG loading) did not significantly improve the proportion of the dose recovered in thoracic lymph over 30h, but predicted uptake over one month was 5 fold greater than the Fab'. This was due to the fact that transit time from the injection site into lymph was approximately 5 fold slower than the Fab'. A possible explanation for this may be that PEGylation resulted in a reduction in receptor mediated, active uptake of Fab' into lymph which would have resulted in slower lymphatic transfer. While no attempt was made to identify a specific receptor for the Fab', HER2 has recently been shown to be expressed on lymphatic endothelial cells[37], providing support for the suggestion of reduced active uptake of Fab' into the lymph following PEGylation. Lymphatic uptake of the 40 kDa

PEG-Fab' was slightly, but not significantly, faster than for the 10 kDa PEG-Fab' and recovery in thoracic lymph was approximately two fold greater. This may have been due to the larger PEG improving the stability of the Fab' at the interstitial injection site, as well as aiding convective transport through the interstitial space and drainage from the site[21].

In conclusion, this study described for the first time the lymphatic pharmacokinetics of a Fab' molecule and the impact of conjugation with 10 and 40 kDa linear PEG chains on the target binding affinity, in vitro activity and lymphatic exposure of the Fab' after IV and SC dosing (6 and 1% respective cumulative recovery in thoracic duct lymph over 30 h). In general, the Fab' displayed similar receptor binding affinity and in vitro anti-proliferative activity when compared to the mAb, but limited lymphatic exposure after IV and SC administration. In contrast, the full length mAb was previously shown to efficiently target lymph after IV and SC administration (44% and 27% respective cumulative recovery in thoracic duct lymph over 30 h)[5]. Site specific conjugation of 10 or 40 kDa linear PEG chains onto the hinge region reduced HER2 binding affinity by 3-4 fold, although in vitro anti-proliferative activity was preserved when compared to unconjugated Fab'. Population pharmacokinetic modeling of the data suggested that the conjugation of 10 kDa PEG (giving approximately 20% PEG loading) increased lymphatic exposure of the Fab' by 5 fold when compared to Fab', although the rate of transfer into peripheral and central lymph was slower when compared to Fab'. Lymphatic exposure after IV administration was estimated to be enhanced by approximately 11 fold. By further increasing PEG loading to 45% (via the conjugation of 40 kDa PEG), lymphatic exposure after SC administration was doubled when compared to the 10 kDa PEG-Fab', but lymphatic exposure after IV administration was not significantly improved. This data collectively suggested that PEGylation can enhance the lymphatic exposure and activity of Fab's against lymph-resident diseases, but that no significant benefit was gained by increasing PEG loading beyond approximately 20%. The data also suggested that the lymphatic exposure and activity of antibody-based therapeutics against

lymph-resident diseases may be greatest for full length mAbs which display better receptor binding affinity and two to three fold greater lymphatic exposure over 30 h when compared to PEGylated Fab' fragments examined here. The selection of Fab or mAb-based therapeutics, however, needs to be evaluated in the context of the specific advantages and disadvantages of each approach in relation to the intended target disease.

Acknowledgements

We thank Dr. Mark Waltham from St Vincent's Hospital for his generous gift of the BT474 breast cancer cells. L.M.K. was supported by an NHMRC Career Development fellowship (APP1022732). D.B.A. was supported by an NHMRC CJ Martin fellowship (APP1072476). J.B.B. is the recipient of an NHMRC Career Development fellowship (APP1084163). C.B.L. is the recipient of an NHMRC Career Development fellowship (APP1062509). This work was supported by an NHMRC project funding grant (APP1044802).

Supporting Information

Figure S1 – SDS-PAGE gel of trastuzumab, trastuzumab Fab' and mono-PEGylated Fab's following staining with coomassie (for protein) and barium iodide (for PEG). Figure S2 – Individual population fits for rats administered Fab' and PEGylated Fab's after IV administration. Figure S2 – Individual population fits for rats administered Fab' and PEGylated Fab's after SC administration.

References

1. Nelson, A. L.; Dhimolea, E.; Reichert, J. M. Development trends for human monoclonal antibody therapeutics. *Nat Rev Drug Discov* **2010,** *9*, (10), 767-74.
2. Chames, P.; Van Regenmortel, M.; Weiss, E.; Baty, D. Therapeutic antibodies: successes, limitations and hopes for the future. *Br J Pharmacol* **2009,** *157*, (2), 220-33.
3. Chapman, A. P. PEGylated antibodies and antibody fragments for improved therapy: a review. *Adv Drug Deliv Rev* **2002,** *54*, (4), 531-45.
4. Wang, W.; Wang, E. Q.; Balthasar, J. P. Monoclonal antibody pharmacokinetics and pharmacodynamics. *Clin Pharmacol Ther* **2008,** *84*, (5), 548-58.
5. Dahlberg, A. M.; Kaminskas, L. M.; Smith, A.; Nicolazzo, J. A.; Porter, C. J. H.; Bulitta, J. B.; McIntosh, M. P. The lymphatic system plays a major role in the intravenous and subcutaneous pharmacokinetics of trastuzumab in rats. *Mol Pharmaceutics* **2014,** *11*, (2), 496-504.
6. Chan, L. J.; Bulitta, J. B.; Ascher, D. B.; Haynes, J. M.; McLeod, V. M.; Porter, C. J.H.; Williams, C. C.; Kaminskas, L. M. PEGylation does not significantly change the initial intravenous or subcutaneous pharmacokinetics or lymphatic exposure of trastuzumab in rats but increases plasma clearance after subcutaneous administration. *Mol Pharmaceutics* **2015,** *12*, (3), 794-809.
7. Weiner, L. M.; Surana, R.; Wang, S. Monoclonal antibodies: versatile platforms for cancer immunotherapy. *Nat Rev Immunol* **2010,** *10*, (5), 317-27.
8. Faulds, D.; Sorkin, E. M. Abciximab (c7E3 Fab). A review of its pharmacology and therapeutic potential in ischaemic heart disease. *Drugs* **1994,** *48*, (4), 583-98.
9. Rosenfeld, P. J.; Brown, D. M.; Heier, J. S.; Boyer, D. S.; Kaiser, P. K.; Chung, C. Y.; Kim, R. Y.; Group, M. S. Ranibizumab for neovascular age-related macular degeneration. *N Engl J Med* **2006,** *355*, (14), 1419-31.
10. Melmed, G. Y.; Targan, S. R.; Yasothan, U.; Hanicq, D.; Kirkpatrick, P. Certolizumab pegol. *Nat Rev Drug Discov* **2008,** *7*, (8), 641-2.
11. Chapman, A. P.; Antoniw, P.; Spitali, M.; West, S.; Stephens, S.; King, D. J. Therapeutic antibody fragments with prolonged in vivo half-lives. *Nat Biotechnol* **1999,** *17*, (8), 780-3.
12. Nelson, A. L. Antibody fragments: hope and hype. *MAbs* **2010,** *2*, (1), 77-83.
13. Humphreys, D. P.; Heywood, S. P.; Henry, A.; Ait-Lhadj, L.; Antoniw, P.; Palframan, R.; Greenslade, K. J.; Carrington, B.; Reeks, D. G.; Bowering, L. C.; West, S.; Brand, H. A. Alternative antibody Fab' fragment PEGylation strategies: combination of strong reducing agents, disruption of the interchain disulphide bond and disulphide engineering. *Protein Eng Des Sel* **2007,** *20*, (5), 227-34.
14. Neuber, T.; Frese, K.; Jaehrling, J.; Jager, S.; Daubert, D.; Felderer, K.; Linnemann, M.; Hohne, A.; Kaden, S.; Kolln, J.; Tiller, T.; Brocks, B.; Ostendorp, R.; Pabst, S. Characterization and screening of IgG binding to the neonatal Fc receptor. *MAbs* **2014,** *6*, (4), 928-42.
15. Trevaskis, N. L.; Kaminskas, L. M.; Porter, C. J. H. From sewer to saviour - targeting the lymphatic system to promote drug exposure and activity. *Nat Rev Drug Discov* **2015,** *14*, (11), 781-803.
16. Schlapschy, M.; Binder, U.; Borger, C.; Theobald, I.; Wachinger, K.; Kisling, S.; Haller, D.; Skerra, A. PASylation: a biological alternative to PEGylation for extending the plasma half-life of pharmaceutically active proteins. *Protein Eng Des Sel* **2013,** *26*, (8), 489-501.
17. Monfardini, C.; Veronese, F. M. Stabilization of substances in circulation. *Bioconjug Chem* **1998,** *9*, (4), 418-50.
18. Kaminskas, L. M.; Ascher, D. B.; McLeod, V. M.; Herold, M. J.; Le, C. P.; Sloan, E. K.; Porter, C. J. H. PEGylation of interferon alpha2 improves lymphatic exposure after subcutaneous and intravenous administration and improves antitumour efficacy against lymphatic breast cancer metastases. *J Control Release* **2013,** *168*, (2), 200-8.
19. Jain, R. K. Physiological barriers to delivery of monoclonal antibodies and other macromolecules in tumors. *Cancer Res* **1990,** *50*, (3 Suppl), 814s-819s.

20. Yokota, T.; Milenic, D. E.; Whitlow, M.; Schlom, J. Rapid tumor penetration of a single-chain Fv and comparison with other immunoglobulin forms. *Cancer Res* **1992,** *52*, (12), 3402-8.
21. Koussoroplis, S. J.; Paulissen, G.; Tyteca, D.; Goldansaz, H.; Todoroff, J.; Barilly, C.; Uyttenhove, C.; Van Snick, J.; Cataldo, D.; Vanbever, R. PEGylation of antibody fragments greatly increases their local residence time following delivery to the respiratory tract. *J Control Release* **2014,** *187*, 91-100.
22. McLennan, D. N.; Porter, C. J. H.; Edwards, G. A.; Martin, S. W.; Charman, S. A. Molecular weight is a primary determinant for lymphatic absorption of proteins following subcutaneous administration to sheep. *AAPS PharmSci* **2002,** *4*, W4041.
23. Kaminskas, L. M.; Kota, J.; McLeod, V. M.; Kelly, B. D.; Karellas, P.; Porter, C. J. H. PEGylation of polylysine dendrimers improves absorption and lymphatic targeting following SC administration in rats. *J Control Release* **2009,** *140*, (2), 108-16.
24. Ascher, D. B.; Wielens, J.; Nero, T. L.; Doughty, L.; Morton, C. J.; Parker, M. W. Potent hepatitis C inhibitors bind directly to NS5A and reduce its affinity for RNA. *Sci Rep* **2014,** *4*, 4765.
25. Kaminskas, L. M.; Kelly, B. D.; McLeod, V. M.; Sberna, G.; Boyd, B. J.; Owen, D. J.; Porter, C. J. H. Capping methotrexate alpha-carboxyl groups enhances systemic exposure and retains the cytotoxicity of drug conjugated PEGylated polylysine dendrimers. *Mol Pharmaceutics* **2011,** *8*, (2), 338-49.
26. Khalili, H.; Godwin, A.; Choi, J. W.; Lever, R.; Brocchini, S. Comparative binding of disulfide-bridged PEG-Fabs. *Bioconjug Chem* **2012,** *23*, (11), 2262-77.
27. Ryan, G. M.; Kaminskas, L. M.; Bulitta, J. B.; McIntosh, M. P.; Owen, D. J.; Porter, C. J.H. PEGylated polylysine dendrimers increase lymphatic exposure to doxorubicin when compared to PEGylated liposomal and solution formulations of doxorubicin. *J Control Release* **2013,** *172*, (1), 128-36.
28. Levy, G. Pharmacologic target-mediated drug disposition. *Clin Pharmacol Ther* **1994,** *56*, (3), 248-52.
29. Mager, D. E.; Jusko, W. J. General pharmacokinetic model for drugs exhibiting target-mediated drug disposition. *J Pharmacokinet Pharmacodyn* **2001,** *28*, (6), 507-32.
30. Bulitta, J. B.; Bingolbali, A.; Shin, B. S.; Landersdorfer, C. B. Development of a new pre- and post-processing tool (SADAPT-TRAN) for nonlinear mixed-effects modeling in S-ADAPT. *AAPS J* **2011,** *13*, (2), 201-11.
31. Bulitta, J. B.; Landersdorfer, C. B. Performance and robustness of the Monte Carlo importance sampling algorithm using parallelized S-ADAPT for basic and complex mechanistic models. *AAPS J* **2011,** *13*, (2), 212-26.
32. Bauer, R. J.; Guzy, S.; Ng, C. A survey of population analysis methods and software for complex pharmacokinetic and pharmacodynamic models with examples. *AAPS J* **2007,** *9*, (1), E60-83.
33. Kawada, K.; Taketo, M. M. Significance and mechanism of lymph node metastasis in cancer progression. *Cancer Res* **2011,** *71*, (4), 1214-8.
34. Ho, R. J.; Yu, J.; Li, B.; Kraft, J. C.; Freeling, J. P.; Koehn, J.; Shao, J. Systems Approach to targeted and long-acting HIV/AIDS therapy. *Drug Deliv Transl Res* **2015**.
35. Sievers, S. A.; Scharf, L.; West, A. P., Jr.; Bjorkman, P. J. Antibody engineering for increased potency, breadth and half-life. *Curr Opin HIV AIDS* **2015,** *10*, (3), 151-9.
36. Jackisch, C.; Muller, V.; Maintz, C.; Hell, S.; Ataseven, B. Subcutaneous Administration of Monoclonal Antibodies in Oncology. *Geburtshilfe Frauenheilkd* **2014,** *74*, (4), 343-349.
37. Mezyk-Kopec, R.; Wyroba, B.; Stalinska, K.; Prochnicki, T.; Wiatrowska, K.; Kilarski, W. W.; Swartz, M. A.; Bereta, J. ADAM17 Promotes Motility, Invasion, and Sprouting of Lymphatic Endothelial Cells. *PLoS One* **2015,** *10*, (7), e0132661.

Tables

Table 1: Noncompartmental pharmacokinetic parameters for Fab', 10 kDa PEG-Fab' and 40 kDa PEG-Fab'. Data are represented as mean ± SD (n = 3-4).

		Fab'				10 kDa PEG-Fab'				40 kDa PEG-Fab'			
		IV	SC	IV-lymph cannulated	SC-lymph cannulated	IV	SC	IV-lymph cannulated	SC-lymph cannulated	IV	SC	IV-lymph cannulated	SC-lymph cannulated
T_{max}	h	0.03 ± 0.0	3.5 ± 0.6	0.03 ± 0.0	2.8 ± 0.5	0.16 ± 0.08	7.5 ± 1.0	0.10 ± 0.04	7.0 ± 1.2	0.12 ± 0.10	25.5 ± 3.0	0.16 ± 0.16	24.0 ± 0.0
C_{max} [b]	mg/L	28.5 ± 7.4	0.6 ± 0.03	30.7 ± 5.1	1.2 ± 0.3	90.9 ± 28.4	2.3 ± 0.5	72.0 ± 10.1	0.7 ± 0.4	70.3 ± 16.0	6.9 ± 0.8	36.9 ± 8.5	1.3 ± 1.1
$t_{1/2}$	h	1.6 ± 0.5	3.1 ± 0.2	2.5 ± 0.5	2.6 ± 0.2	24.1 ± 11.1	25.6 ± 9.4	[a]	[a]	32.0 ± 3.3	38.4 ± 9.5	[a]	[a]
$AUC_{0\text{-}30h}$ [b]	mg/L.h	9.0 ± 2.5	4.7 ± 0.5	11.9 ± 1.7	7.8 ± 2.1	271 ± 56.6	51.8 ± 17.2	244 ± 54.9	15.3 ± 7.1	765 ± 78.8	115 ± 25.8	266 ± 37.5	23.5 ± 16.6
$AUC_{0\text{-}\infty}$ [b]	mg/L.h	9.0 ± 2.5	4.7 ± 0.5	11.9 ± 1.7 [a]	7.8 ± 2.1	293 ± 67.5	92.2 ± 36.7	[a]	[a]	1310 ± 163	545 ± 140	[a]	[a]
CL[c]	mL/h	62.9 ± 17.7	114 ± 11.4	45.2 ± 6.3	72.1 ± 21.9	1.9 ± 0.4	6.3 ± 1.9	2.3 ± 0.7	28.3 ± 11.7	0.4 ± 0.06	1.0 ± 0.3	1.7 ± 0.3	14.0 ± 14.2
F_{lymph}	%			1.3 ± 0.4	6.4 ± 3.4			15.1 ± 2.3	8.6 ± 1.7			14.0 ± 8.9	18.1 ± 10.4

Cmax: observed maximum concentration in plasma,
Tmax: time of Cmax,
$t_{1/2}$: terminal half-life,
$AUC_{0\text{-}30h}$: area under the plasma concentration time curve from time 0 to 30 h,
$AUC_{0\text{-}\infty}$: area under the plasma concentration time curve from time 0 h to infinity,
F_{lymph}: fraction of dose recovered in lymph over 30 h
CL: total body clearance.

[a]: Unable to be calculated since a clear elimination phase was not evident over 30h
[b]: Values were normalized to an average dose of 0.561 mg.
[c]: Represents CL/F, where F is bioavailability, for SC administration
One-way ANOVA was performed to compare the corresponding PK parameters for three Fab' constructs.

* significant (p-value; 0.01 to 0.05), **very significant (p-value: 0.001 to 0.01), ***extremely significant (p-value: 0.0001 to 0.001), ***extremely significant (p-value <0.0001), ns: not significant

Non-lymph cannulated: **IV:** T_{max}* C_{max}*, $t_{1/2}$**, $AUC_{0\text{-}30h}$****, $AUC_{0\text{-}\infty}$ ****, CL***. **SC:** T_{max}****, C_{max}****, $t_{1/2}$**, $AUC_{0\text{-}30h}$***, AUC0-∞ ***, CL****

Lymph cannulated: **IV:** T_{max} ^{ns}, C_{max}**, $AUC_{0\text{-}30h}$***, CL****, F_{lymph}*. **SC:** T_{max}**** C_{max} ^{ns}, $AUC_{0\text{-}30h}$ ^{ns}, CL*, F_{lymph} ^{ns}.

Table 2: Estimated population pharmacokinetic model parameters for Fab', 10kDa PEG-Fab' and 40 kDa PEG-Fab' in Sprague-Dawley rats.

Parameter	Symbol	Unit	Population means (SE%)			Between subject variability (SE%)		
			Fab'	10 kDa PEG-Fab'	40 kDa PEG-Fab'	Fab'	10 kDa PEG-Fab'	40 kDa PEG-Fab'
Fraction absorbed into plasma after SC dosing	F_{PL}		0.793 (24.1%)	0.118 (21.1%)	0.628 (9.75%)	0.231 (97.7%)[a]	0.279 (89.4%)[a]	0.091 (201%)[a]
Fraction absorbed into lymph after SC dosing	F_{LY}		0.0347 (54.1%)	0.183 (47.2%)	0.326 (42.1%)	0.715 (124%)	0.427 (105%)	0.502 (79.3%)
Clearance	CL	mL/h	42.1 (4.67%)	1.75 (8.46%)	0.296 (4.97%)	0.131 (218%)	0.129 (152%)	0.053 (110%)
Distribution clearance	CL_D	mL/h	3.63 (51.6%)	4.97 (17.7%)	0.328 (37.4%)	0.552 (123%)	0.236 (115%)	0.523 (130%)
Volume of distribution of central compartment	V_1	mL	13.5 (0.967%)	7.11 (10.3%)	13.1 (12.4%)	0.014 (272%)	0.214 (135%)	0.316 (88%)
Volume of distribution of peripheral compartment	V_2	mL	25.7 (5.73%)	3.00 (13.9%)	6.74 (3.26%)	0.090 (220%)	0.147 (234%)	0.024 (191%)
Mean transit time (MTT) from the SC injection site to the central compartment (plasma)	$MTT_{1a2}^{b,c}$	h	4.74 (2.08%)	32.0 (29.7%)	486 (61.6%)	0.017 (111%)	1.02 (88.9%)	1.47 (53%)
MTT from the SC injection site to posterior peripheral lymph	$MTT_{1b4}^{b,c}$	h	3.60 (1.82%)	16.8 (5.09%)	15.5 (28.3%)	0.012 (132%)	0.071 (157%)	0.711 (88%)
MTT from central compartment to peripheral lymph	$MTT_{24}^{b,c}$	h	18.4 (9.07%)	19.5 (0.657%)	105 (13.1%)	0.096 (167%)	0.005 (266%)	0.679 (117%)
MTT from peripheral lymph to central lymph	$MTT_{45}^{b,c}$	h	1.16 (3.24%)	5.15 (35.8%)	3.55 (44.8%)	0.029 (210%)	1.15 (77.7%)	1.18 (63%)
MTT from central lymph to central compartment	$MTT_{52}^{b,c}$	min	10 (fixed)	10 (fixed)	10 (fixed)			

Concentration of receptor at time 0 h	$C_{Rec,0}$	mg/L	6.23 (13.2%) [d]	6.23 (13.2%) [d]	6.23 (13.2%) [d]	0.606 (51.8%)	0.606 (51.8%)	0.606 (51.8%)
Association rate constant	k_{on}	L/(mg·h)	2.69 (11.6%)	0.0158 (25.9%)	0.0126 (27%)	0.150 (fixed)	0.150 (fixed)	0.150 (fixed)
Dissociation half-life	$\ln(2)/k_{off}$	d	4.45 (24%)	1.30 (17.5%)	1.22 (25.7%)	0.150 (fixed)	0.150 (fixed)	0.150 (fixed)
Degradation half-life for receptor	$\ln(2)/k_{deg}$	d	0.700 (6.27%)	0.700 (6.27%)	0.700 (6.27%)	0.046 (240%)	0.046 (240%)	0.046 (240%)
Elimination half-life for drug-receptor complex	$\ln(2)/k_{int}$	d	1.10 (63.1%)	1.10 (63.1%)	1.10 (63.1%)	0.475 (131%)	0.475 (131%)	0.475 (131%)

SE%: Relative standard error. The standard deviation of the additive residual error for the plasma concentrations was 17.2 ng/mL for Fab', 10.7 ng/mL for the 10 kDa PEG-Fab', and 27.4 ng/mL for the 40 kDa PEG-Fab'. The coefficient of variation of the proportional residual error for the plasma concentrations was 12.5% for Fab', 21.0% for the 10 kDa PEG-Fab', and 18.3% for the 40 kDa PEG-Fab'. The standard deviation of the additive residual error for the fraction of dose in lymph was 0.0463% for Fab', 0.556% for the 10 kDa PEG-Fab', and 0.0139% for the 40 kDa PEG-Fab'. The coefficient of variation of the proportional residual error for the fraction of dose in lymph was 41.8% for Fab', 43.1% for the 10 kDa PEG-Fa'b, and 55.0% for the 40 kDa PEG-Fab'.

[a]: The estimate represents the apparent coefficient of variation of a normal distribution on natural log-scale and the estimate in parenthesis is the relative standard error of the estimated variance on natural log-scale.

[b]: The mean transit times were estimated via modeling. The rate constants shown in Figure 7 were calculated as the inverse of these mean transit time (*e.g.* $k_{1a2} = 1 / MTT_{1a2}$).

[c]: Assuming that the distribution to the anterior and posterior lymph loop were comparably fast, k_{26} was fixed to the estimate of k_{24}, k_{67} was fixed to the estimate of k_{45}, and k_{72} was fixed to the value of k_{52}.

[d]: The differential equations were calculated using units of mg/L for all three compounds and of mg for the associated amounts of the compounds. As we did not have observed data on the receptor concentration in plasma, we assumed mg/L as the hypothetical unit for the total receptor concentration in plasma.

Table 3: Predicted fractions of dose flowing through the posterior and anterior lymph loops for up to 28 days after intravenous or subcutaneous dosing of 0.531 mg of the three Fab' constructs with and without thoracic lymph duct cannulation

	Fab'				10 kDa PEG-Fab'				40 kDa PEG-Fab'			
Lymph	**IV**	**SC**	**IV-lymph cannulated**	**SC-lymph cannulated**	**IV**	**SC**	**IV-lymph cannulated**	**SC-lymph cannulated**	**IV**	**SC**	**IV-lymph cannulated**	**SC-lymph cannulated**
Posterior	1.43%	4.48%	1.40%	4.41%	19.1%	23.6%	16.1%	20.0%	23.8%	48.6%	19.1%	41.0%
Anterior	1.43%	1.02%	1.40%	0.943%	19.1%	5.30%	16.1%	1.74%	23.8%	16.0%	19.1%	8.38%

Figure captions:

Figure 1: Schematic representation of the preparation of Fab' and mono-PEGylated Fab' using 10 kDa and 40 kDa PEG molecules.

Figure 2: SEC-MALS analysis of the **(A)** 10 kDa PEG-Fab' and **(B)** 40 kDa PEG-Fab'. PEGylated trastuzumab Fab' was monitored by normalised differential refractive index (black line) and absorbance at 280 nm versus time. Molar mass was analysed by multi-angle light scattering following the total mass by differential refractive index (blue points), and protein mass by absorbance at 280 nm (grey points). The molar mass contributed by PEGylation is plotted as the difference between the total mass and the mass of the protein (orange points).

Figure 3: Binding of Fab' and PEGylated Fab' to HER2. Values on the Y axis represent the percentage of the maximal thermophoretic response (MST) observed. All binding curves were determined in triplicate by MST and are represented as the mean ± SD.

Figure 4: In vitro growth inhibition of BT474 human breast cancer cells by Fab' and PEGylated Fab'. Growth inhibition curves were fitted using a sigmoidal dose-response (inhibition) curve on GraphPad Prism. Values are expressed as mean ± SD (n = 3).

Figure 5: Plasma concentration-time profiles and population fits (popfit) of Fab' and PEGylated Fab's in control (●) and thoracic lymph duct-cannulated (○) rats dosed IV (panels A-C) and SC (panels D-F) at 2 mg/kg. IV Fab' (panel A), IV 10 kDa PEG-Fab' (panel B), IV 40 kDa PEG-Fab' (panel C), SC Fab' (panel D), SC 10 kDa PEG-Fab' (panel E), SC 40 kDa PEG-Fab' (panel F). Data is represented as mean ± SD (n = 4). * Represents a significant difference at the indicated time points between control and lymph cannulated groups using two-way ANOVA.

Figure 6: Cumulative lymph profiles and population fits (popfit) from thoracic lymph duct-cannulated rats over 30 h after IV (panel A) and SC (panel B) administration of Fab' and PEGylated Fab's, Data is represented as mean ± SD (n = 4).

Figure 7: Structure of the mechanism-based model for Fab' and PEGylated Fab's in rats. After SC injection, a fraction of the dose was assumed to enter the central compartment and another fraction to enter the posterior, peripheral lymph compartment via first-order processes. All three constructs could be described by the same structural model, however, target-mediated drug disposition (TMDD) was most pronounced for the Fab'. The drug in the central compartment was assumed to reversibly bind to the receptor with rate constants k_{on} and k_{off}. Receptor synthesis and degradation as well as the elimination of the drug-receptor complex were included in the model.

Figures:

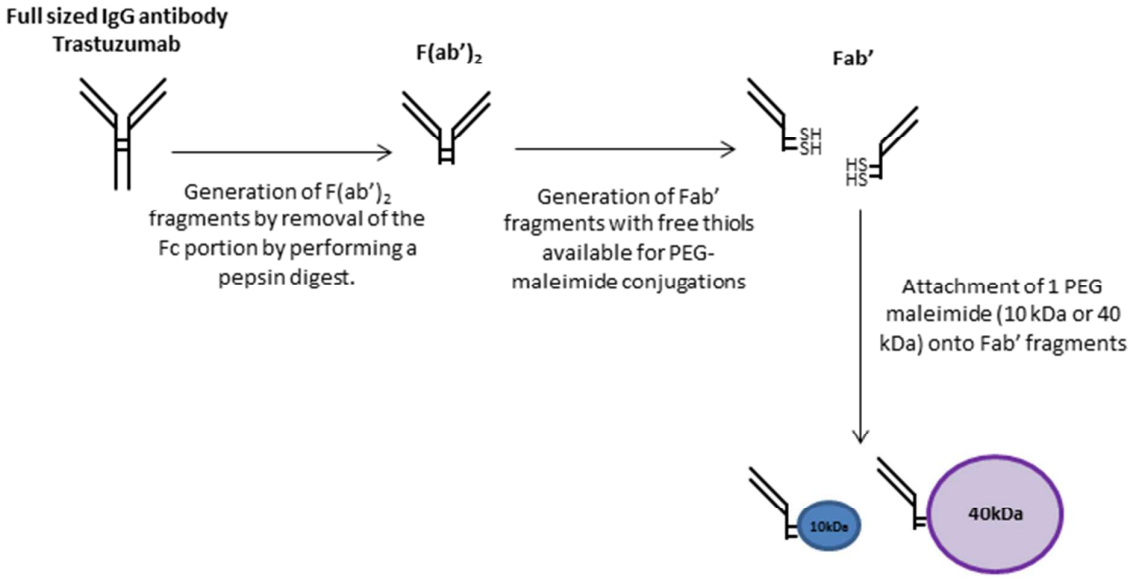

Figure 1

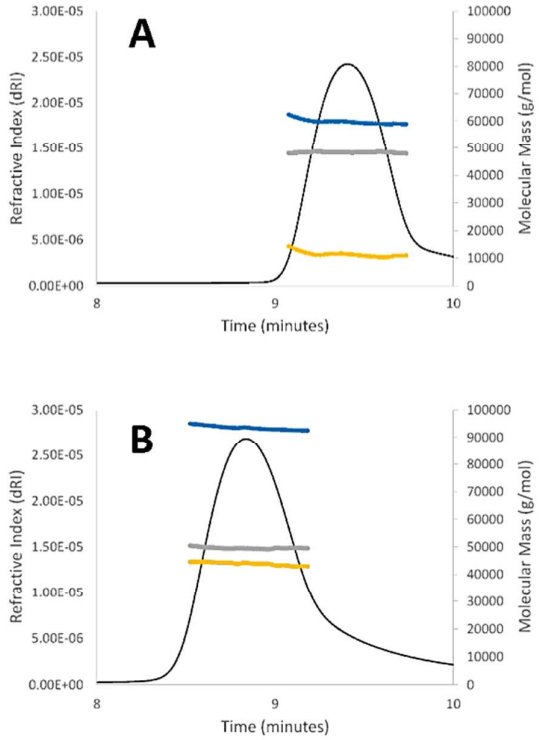
A
Refractive Index (dRI)
Molecular Mass (g/mol)
Time (minutes)
3.00E-05
2.50E-05
2.00E-05
1.50E-05
1.00E-05
5.00E-06
0.00E+00
100000
90000
80000
70000
60000
50000
40000
30000
20000
10000
0
8
9
10
B
Refractive Index (dRI)
Molecular Mass (g/mol)
Time (minutes)

Figure 2

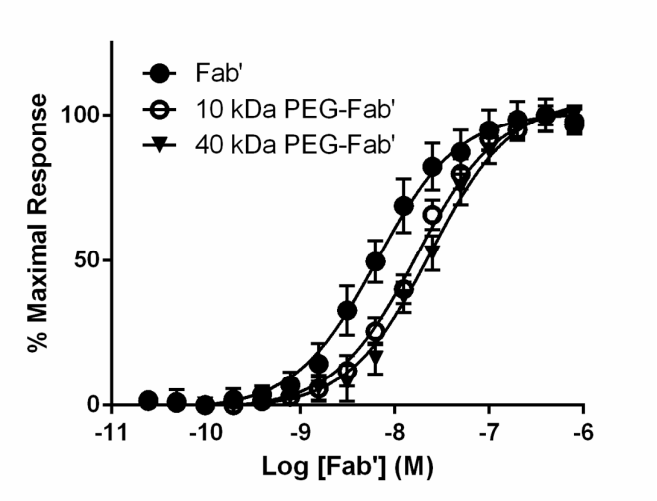
Fab'
10 kDa PEG-Fab'
40 kDa PEG-Fab'
% Maximal Response
100
50
0
-11
-10
-9
-8
-7
-6
Log [Fab'] (M)

Figure 3

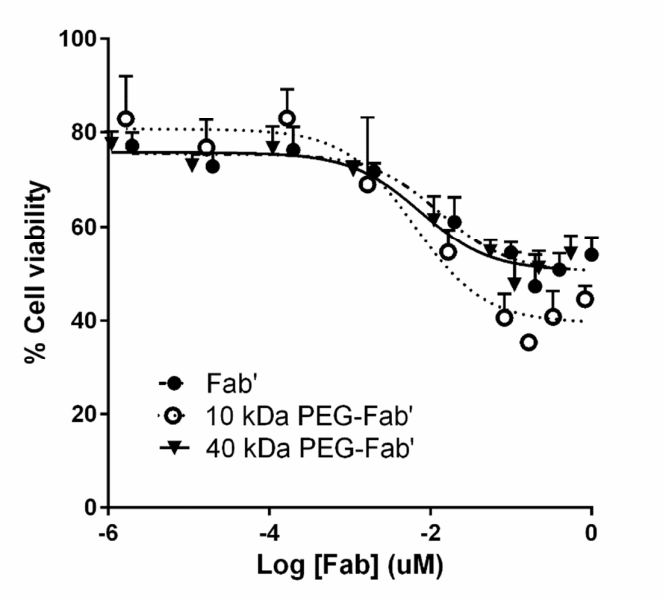
100
80
60
40
20
0
% Cell viability
-6
-4
-2
0
Log [Fab] (uM)
Fab'
10 kDa PEG-Fab'
40 kDa PEG-Fab'

Figure 4

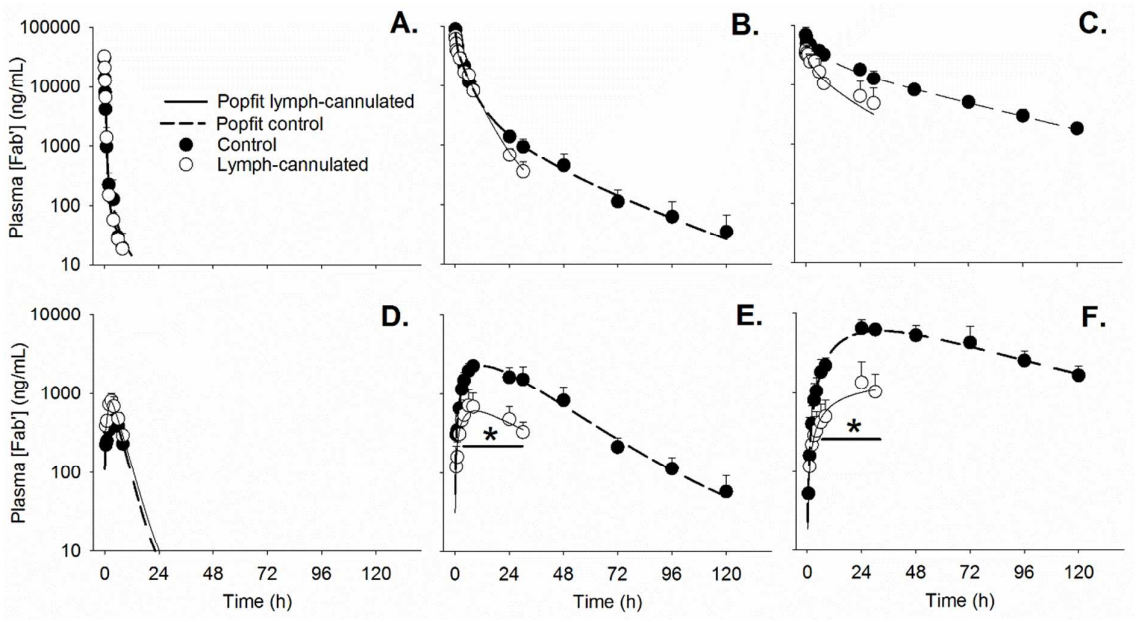
A.
B.
C.
D.
E.
F.
Plasma [Fab'] (ng/mL)
100000
10000
1000
100
10
Popfit lymph-cannulated
Popfit control
Control
Lymph-cannulated
*
0
24
48
72
96
120
Time (h)

Figure 5

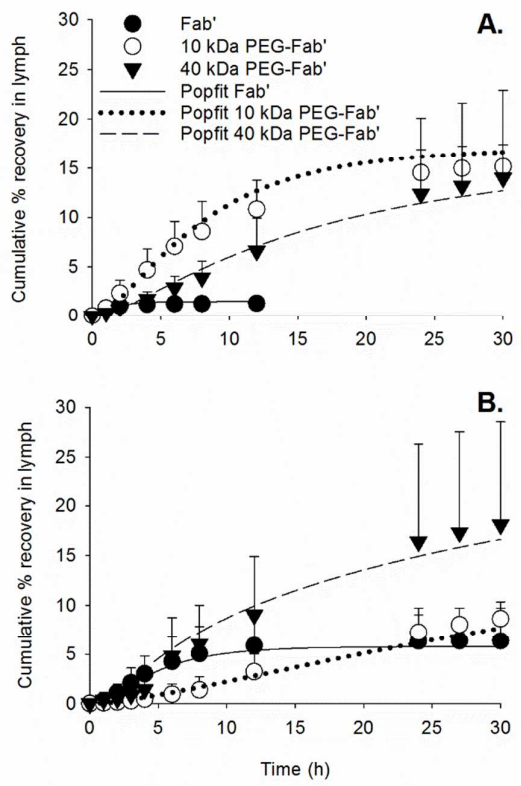
A.
B.
Fab'
10 kDa PEG-Fab'
40 kDa PEG-Fab'
Popfit Fab'
Popfit 10 kDa PEG-Fab'
Popfit 40 kDa PEG-Fab'
Cumulative % recovery in lymph
Cumulative % recovery in lymph
Time (h)
0
5
10
15
20
25
30

Figure 6

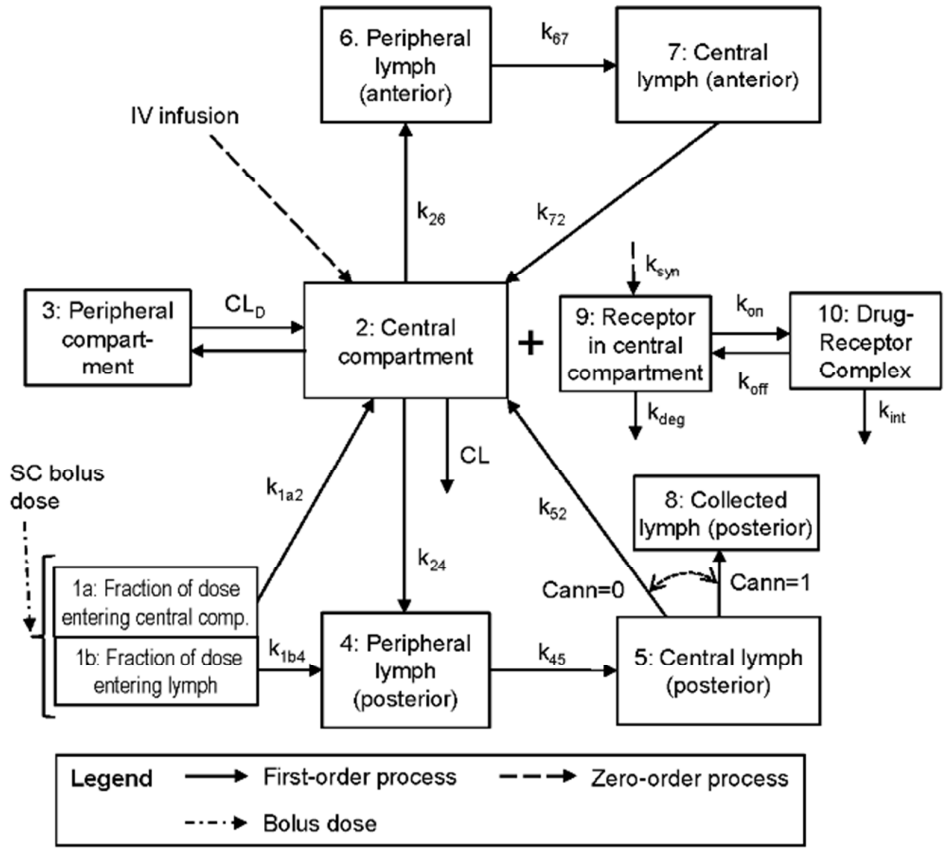
6. Peripheral lymph (anterior)
k_{67}
7: Central lymph (anterior)
IV infusion
k_{26}
k_{72}
k_{syn}
3: Peripheral compart-ment
CL_D
2: Central compartment
9: Receptor in central compartment
k_{on}
k_{off}
10: Drug-Receptor Complex
k_{deg}
k_{int}
CL
SC bolus dose
k_{1a2}
k_{52}
8: Collected lymph (posterior)
k_{24}
Cann=0
Cann=1
1a: Fraction of dose entering central comp.
1b: Fraction of dose entering lymph
k_{1b4}
4: Peripheral lymph (posterior)
k_{45}
5: Central lymph (posterior)
Legend
First-order process
Zero-order process
Bolus dose

Figure 7